Flange-to-flange double-tee connections subjected to vehicular loading, part 1: Numerical assessment approach

Robin Hendricks, Clay Naito, and Andrew Osborn

- PCI-funded research was conducted to assess the fatigue resistance of welded flange-to-flange connections in double-tee precast concrete construction.
- The strength limit states of this connection type have been explored in detail, but the stresses in the connection at cyclic service load levels are not well understood.
- The ability to accurately determine the stresses in the weld can be combined with a vehicular load spectrum and a suitable fatigue-life curve for the fillet weld detail to obtain a realistic assessment of the fatigue life of these connections.

For over 50 years, prestressed concrete double-tee members have been the component of choice for parking structures throughout the United States. The double-tee members are laid side by side and typically span approximately 60 ft (18 m). The 60 ft span is desirable because it provides a column-free span to allow for two drive aisles flanked on both sides by parking stalls. Double-tee floor systems can be topped in the field with cast-in-place concrete or manufactured with the appropriate strength and surface conditions to eliminate the need for field-placed topping. These two types of systems are referred to as topped and untopped (or pretopped) double-tee parking structures. The decks serve not only to support traffic but also to act as diaphragms to distribute lateral loads to frames and shear walls.

Welded plate connections have typically been used to provide lateral continuity between pretopped double tees, away from the ends (**Fig. A1** [for appendix figures, go to www.pci.org/Naito_Appendix]). For pretopped double tees, earlier connections included plant-fabricated plates with headed studs, deformed bar anchors, or welded reinforcing bars that allowed anchorage into the flange. Embedded plates on adjacent double tees were joined using a round bar or a rectangular plate—also called a jumper plate, erection plate, or slug—field welded to the embedded flat plates (**Fig. 2**). Starting around the year 2000,[1] proprietary connection hardware began to be sold in the United States. The original proprietary connections were made from galvanized mild steel. Increasingly, stainless steel connections are used in

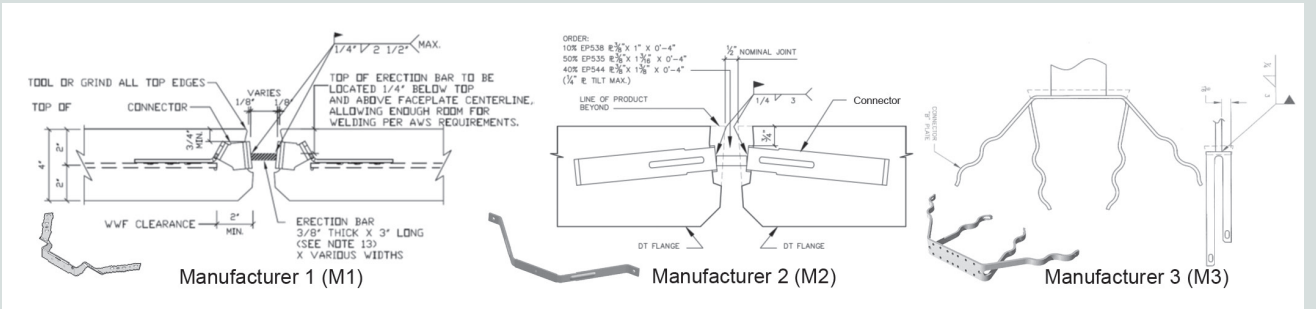

Figure 1. Proprietary connectors currently available in the marketplace. Note: 1" = 1 in. = 25.4 mm; 1' = 1 ft = 0.305 m.

climates where the use of road salts is common. **Figure 1** illustrates three common manufactured connectors used in the United States today.

Manufactured connectors all consist of a faceplate with integral legs that are embedded in the concrete and are connected by a jumper plate with a fillet weld on each side. The fillet weld is applied on the top surface of the jumper plate only, and this configuration can result in bending stresses on the weld throat with the root of the weld in tension. The most common type of jumper plate is 0.375 in. (9.53 mm) thick, 2.5 to 3.5 in. (64 to 89 mm) long, and 0.5 to 2 in. (13 to 50 mm) wide. Round jumper plates of similar dimensions are sometimes used instead of rectangular plates (Fig. A2). Jumper plate widths and diameters are adjusted to accommodate variable joint gaps between double tees but are typically about 1 in. (25 mm) wide. Connections are usually spaced 5 to 8 ft (1.5 to 2.4 m) on center along the joint with closer spacing sometimes used at the midspan of the double tees.

A significant amount of research has been conducted to assess the performance of double-tee flange connections under strength levels. Early testing was performed by Venuti,[2] Spencer and Neille,[3] and Aswad[4] on nonproprietary connections, and testing on manufactured connections was performed by Pincheira et al.;[5] Oliva;[6] Wiss, Janney, Elstner Associates;[7] Shaikh and Fiele,[8] Naito,[9] and Naito and Hendricks.[10] Testing consisted of in-plane shear and tension and out-of-plane shear forces across the joint. Some of the studies are summarized in Ren and Naito.[11] The focus of the majority of these studies was to determine the capacity of the connections for design purposes. In all cases, only one connector was embedded in a concrete panel. The jumper plate was welded to the faceplate and loaded as a short cantilever. Research was also conducted to assess stiffness and ductility relative to in-plane shear and axial loads to assess the response of these connections under seismic demands.[12,13] Due to the complexity of the load path through manufactured connections, experimental testing is conventionally used over closed-form calculations to determine connector strength limit states.[14] Consequently, the detailed mechanics of the individual connectors are not well understood. At service-level loading, research has been limited to studies by Klein and Lindenberg[15] that explored the deformation levels generated in double-tee floor diaphragms

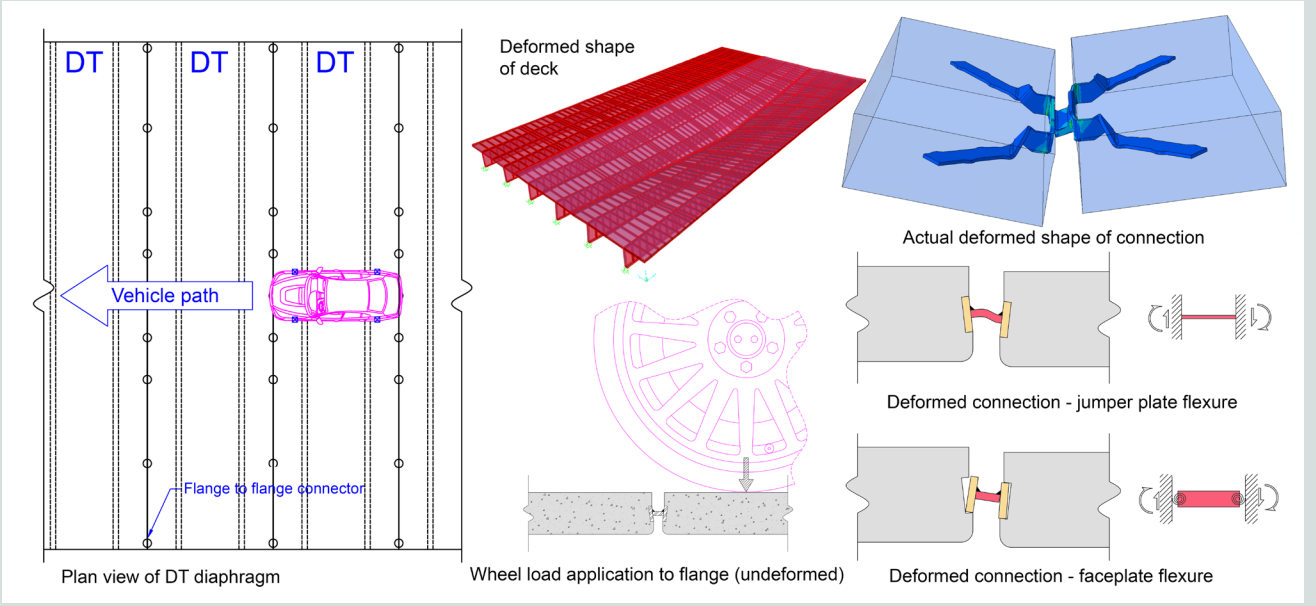

Figure 2. Differential flange deflections due to vehicular loading. Note: DT = double tee.

due to thermal variations. Although significant efforts have been conducted to ensure the performance of connections under strength and thermal limit states, fatigue limit states have not been examined.

Cyclic connector loading arises from differential flange deflections caused by vehicles crossing the flange joints (**Fig. 2**). Proper assessment of the connection for fatigue resistance requires a knowledge of the following:

- the relationship between the applied vehicle load and the resulting stresses in the connection welds
- the expected vehicle demands and distributions in the structure over the expected service life
- an S-N curve—which is a plot of stress versus number of cycles to failure—that is applicable for the weld being considered

With a proper understanding of these three pieces, any combination of connections and vehicle loads can be examined to assess the likelihood of fatigue-induced fracture of connection welds. This paper focuses on the development and validation of a methodology for the determination of weld stresses in connections due to applied vehicle loads.

Connection evaluation methodology

Simple approaches have been used in the past to approximate the strength of connections for design. The first edition of the *PCI Connections Manual for Precast and Prestressed Concrete Construction*,[16] for example, assumes that vehicle loads impart only shear on the connection weld (eccentricity between welds is ignored). Other approaches attempt to incorporate both the shear and resulting flexure that is introduced across the jumper plates. This can range from a case where it is assumed that the jumper plate is rigid and all deformation takes place in the faceplate (Fig. 2) to a case where the faceplate of the connection is assumed rigid and all deformation takes place in the jumper plate (Fig. 2). Due to the relative flexibility of the faceplate and its lack of bond to the surrounding concrete, actual weld and jumper plate response is much more complicated. As illustrated in the finite element analysis in Fig. 2, the stresses that arise in conventional connector systems due to vehicle loading vary in three dimensions and are beyond the scope of traditional hand calculations.

Three-dimensional (3-D) finite element analysis of the entire diaphragm system provides the most accurate modeling approach for assessment of connector response. These models can be complex and computationally expensive. In addition, modeling all discrete connections of an entire deck does not lend itself to assessment of the wide variations in parking structure configurations that are present in current construction. A simplified numerical method is proposed that can be used to accurately determine the stresses in flange-to-flange connection welds (**Fig. A3**). As a first step, the stiffness of the connection is determined from a detailed 3-D finite element model of the local system. In the second step, the connector stiffness is used in a shell model of a diaphragm system with the connectors replaced by linear uncoupled springs to determine the connection deformation under loading. The final step consists of application of the differential displacements and rotations to the initial 3-D finite element model to determine the actual stresses in the weld under loading. These stresses can then be used with an appropriate S-N curve to determine the likelihood of fatigue-induced fracture. The modeling approach proposed is validated by experimental data acquired from full-scale connector component tests and welded-connection double-tee tests.

Development and validation of three-dimensional finite element model

Development of an accurate 3-D finite element model is critical to the approach proposed. Many commercial codes are available for development of such a model; however, due to the complexity of the model, validation is necessary. To examine the accuracy of the 3-D modeling approach, a series of component tests was conducted to measure the response of full-scale connections.

Component tests on full-scale connections

Single-sided connector tests were performed with the goal of calibrating detailed 3-D finite element models of the connectors. The connectors were loaded at an eccentricity of 1.0 in. (25 mm) from the face of the connector, and the applied load, vertical displacement, loading block rotation, and strains in at least three locations were recorded throughout the test. The connectors were loaded in force increments of 300 lb (1300 N) up to 1500 lb (6700 N) and were then monotonically loaded to failure. Three cycles were applied at each force level (that is, 0 to 300 lb [1330 N] three times, 0 to 600 lb [2670 N] three times, and 0 to 900 lb [4000 N], and the like) with application at a quasistatic rate.

The tests evaluated the response of connectors embedded in concrete subjected to vertical shear. Half of the connection was evaluated, in that one embedded connector was tested with a jumper plate and a loading fixture. **Figures 3** and **A4** show the test setup. A 0.375 in. (9.53 mm) thick, 4 in. (100 mm) wide jumper plate was attached to a single embedded connector. The jumper plate was oversized to allow attachment to a loading head. The test fixture was manufactured such that the center of vertical shear was located 1.0 in. from the face of the connector. A series of strain gauges (measuring horizontal strain) were included on the face of the connector, and vertical displacement was measured using a transducer attached to the loading head. Rotation of the loading head was also monitored using a tilt gauge mounted to the loading head as illustrated in Fig. 3.

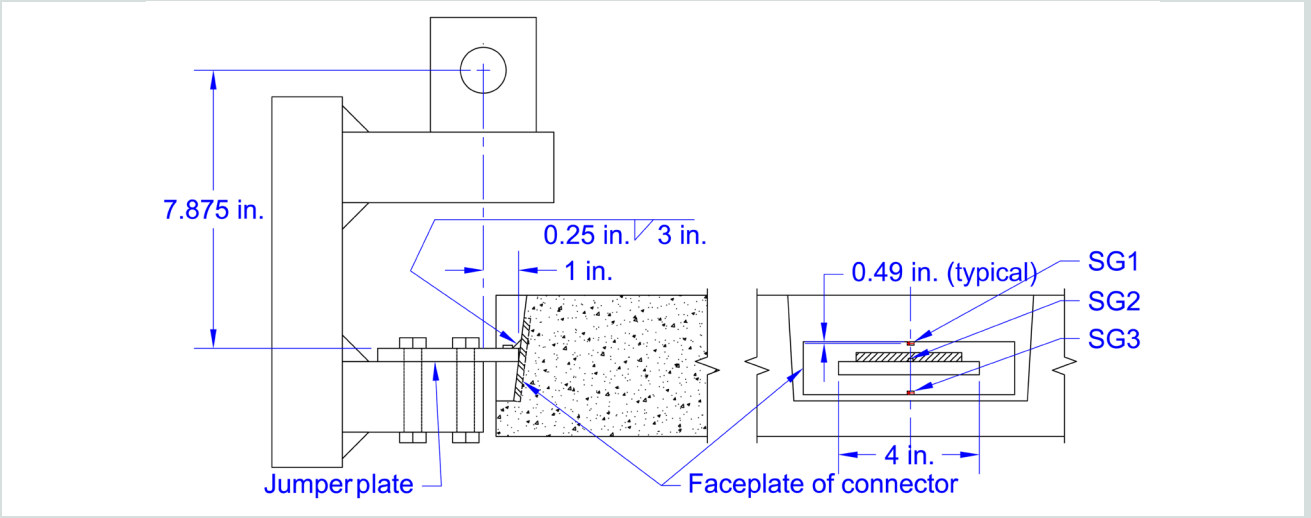

Figure 3. Overall single connector test setup details. Note: 1 in. = 25.4 mm.

Twelve tests were conducted on connectors produced by three connector manufacturers identified as M1, M2, and M3 (Fig. 1). A carbon steel and stainless steel variation of each connector was evaluated. Each connector type was tested once in an upward direction (corresponding to tension at the weld root) and once in a downward direction (corresponding to closing the gap between jumper plate and connector faceplate). These directions represent the general response that would occur on the left and right sides of the jumper plate due to vertical loading (Fig. 2). **Table 1** presents the test results. Concrete compression tests were conducted prior to the start of the testing program and at the end of the testing program in accordance with ASTM C39.[17] The concrete compressive strength ranged from 5700 to 6230 psi (39.3 to 43.0 MPa) for the carbon steel connection tests and from 5510 to 5980 psi (38.0 to 41.2 MPa) for the stainless steel connection tests. The concrete compressive strength for each connector test was linearly interpolated based on the age of the panel relative to the cylinder test dates, as summarized in Table 1. The strength of the connector in each direction is noted along with the associated deformation. Due to a varying initial stiffness, the applied load at a deformation of 0.010 in. is reported in lieu of an initial stiffness.

Table 1. Summary of results

Connector	Direction	Estimated compressive strength, psi	Applied load at deformation of 0.010 in., lb	Maximum strength, lb	Deformation at maximum strength, in.
M1 carbon	Upward	5970	199	4418	0.119
	Downward	5980	398	7513	0.092
M2 carbon	Upward	6550	1040	6270	1.225
	Downward	5900	195	6573	0.123
M3 carbon	Upward	5900	294	7191	0.285
	Downward	5910	365	6828	0.118
M1 stainless	Upward	5900	287	5084	0.121
	Downward	5940	143	6681	0.148
M2 stainless	Upward	5800	259	8186	1.166
	Downward	5960	110	9174	0.564
M3 stainless	Upward	5950	773	8241	0.274
	Downward	5950	597	7674	0.138

Note: 1 in. = 25.4 mm; 1 lb = 4.448 N; 1 psi = 6.895 kPa.

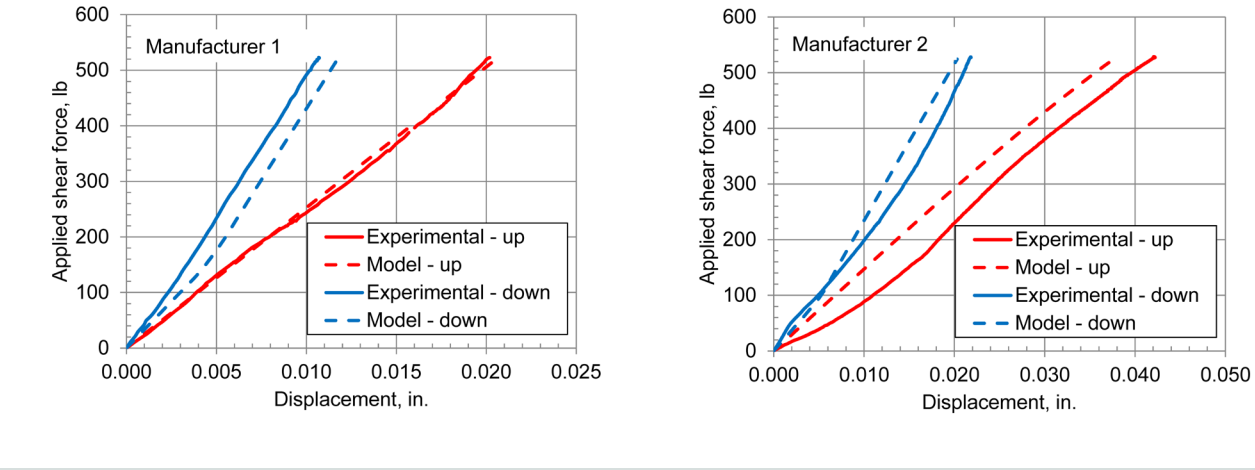

Figure 4. Comparison of numerical model with measured results for single-sided loading. Note: 1 in. = 25.4 mm; 1 lb = 4.448 N.

The vertical load deformation of the connections in the upward direction is positive and the downward direction is negative for the carbon and stainless steel connections (**Fig. A5**). A detailed summary of each test is provided in Naito and Hendricks.[18] Variation in response between connectors and material types may be attributed to differences in connector geometry.

Three-dimensional numerical model development

The connectors were tested individually, as noted, and were initially modeled as single-sided to verify the accuracy of the finite element model. Based on observations of the elastic performance in the experiments, the concrete remained undamaged at the loads of interest. Two model types were created to compare with the test data. A complete detail incorporating concrete embedment and contact was used for manufacturer 1, and a simplified approach was used to represent the embedment for manufacturer 2 (**Fig. 6**). The simplified approach facilitates rapid assessment and requires less modeling time. The simple assembly consists of a 3-D model of the connector. Any locations where concrete embedment would be present are replaced with elastic supports. A rigid block is included to model the contact between the back of the connector face and the concrete. Nodal ties were used to join the weld to the connector face and to the jumper plate. Hard contact with no friction was used to model the contact between the connector and concrete and between the jumper plate and the connector face.

In the second model, the 3-D connector mesh is embedded in 3-D concrete mesh. Connectivity between the concrete and steel elements was accomplished through nodal ties up to the point where the connector legs return to the face of the concrete. The contact interactions between the jumper plate and connector and between the connector faceplate and concrete were modeled using frictionless hard contact. Bond between the concrete and connectors is assumed to be negligible for both models due to the smooth zinc coatings used and is not included. All models were meshed with quadratic brick elements for the connector and jumper plate geometry and with quadratic tetrahedral elements for the concrete. All material properties used in the model were linear elastic, with a modulus of elasticity of 29,000 ksi (200 GPa) and a Poisson's ratio of 0.3. The concrete was modeled using an elastic modulus of 4400 ksi (30 MPa) and a Poisson's ratio of 0.15.

Three-dimensional numerical model validation

The connection assemblies were modeled with load applied in upward and downward directions to match the experimental program. The measured vertical force versus measured vertical deflection results were compared with the model results up to an applied vertical force of 525 lb (2340 N). The model shows good agreement for connectors from both manufacturers 1 and 2 (**Fig. 4**). The measured strains from gauges SG1, SG2, and SG3 (Fig. 3) versus measured vertical deflection are compared with the modeled values for vertical deflections in the same range of applied load. **Figures 5** and **A6** compare the experimental strain measurements with the models for manufacturer 1 and 2, respectively. In general, data from strain gauges SG1, SG2, and SG3 compare well between the model and the experimental data. The accuracy of the model in computing both the global behavior and the local strains (less than 20% error) validates the accuracy of both the simplified and complex modeling approaches.

Determination of connection stiffness

The finite element models were extended from the single-sided connection to the full flange-to-flange connection. The model was created by combining the upward and downward load models from manufacturer 1 into a single assembly. The contact interactions between the two models were consistent with the single-sided model used for connection M1. The connector

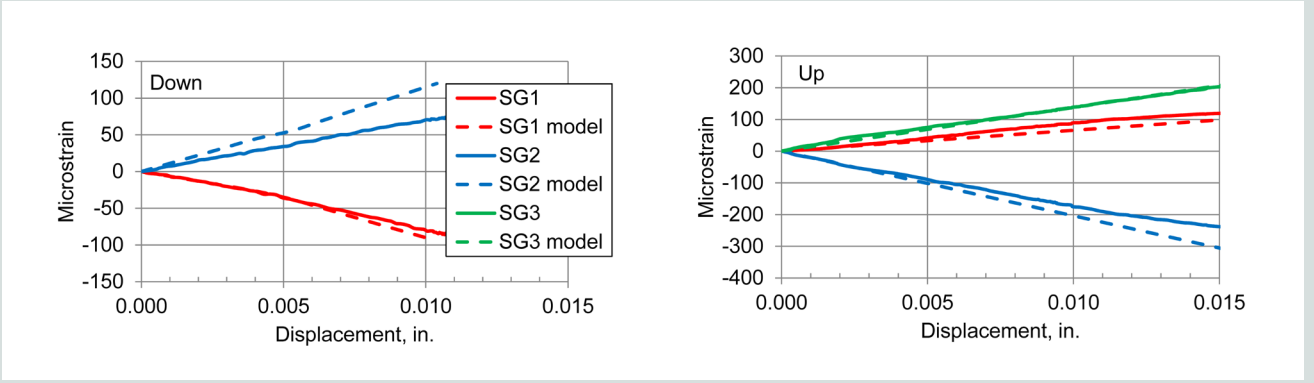

Figure 5. Comparison of numerical model with strain-displacement experimental results for manufacturer 1. Note: 1 in. = 25.4 mm.

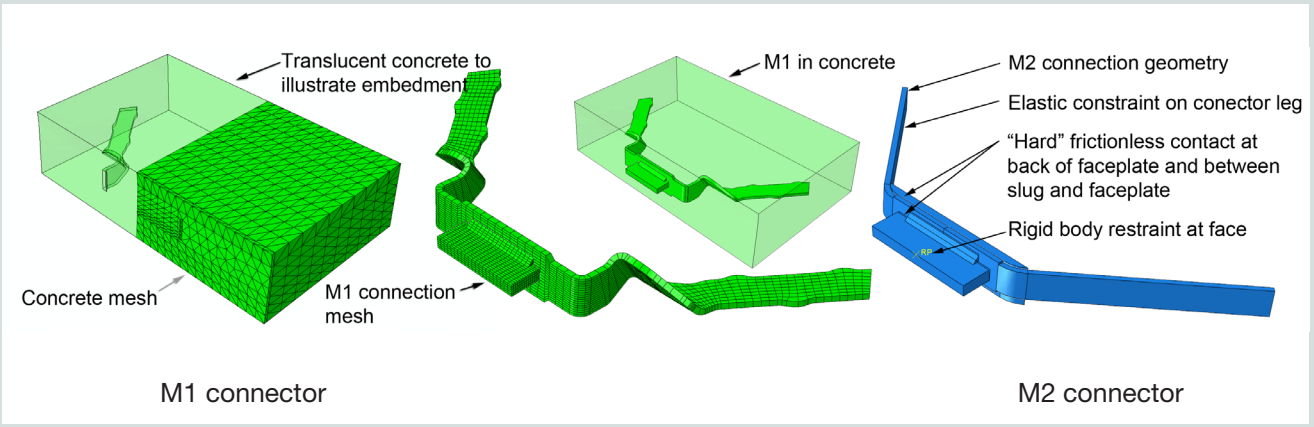

Figure 6. Three-dimensional finite element model details.

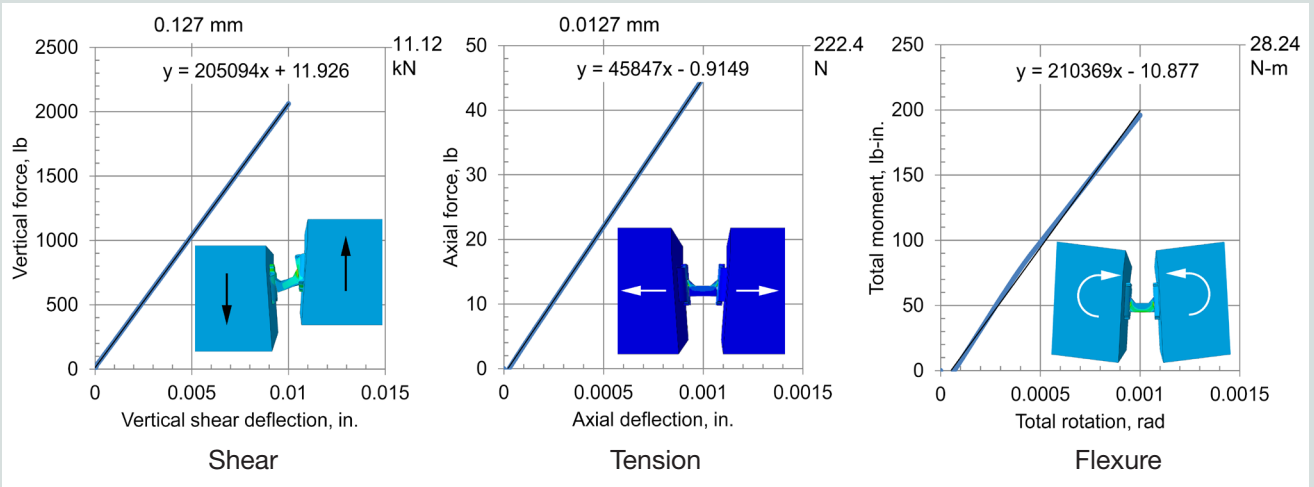

Figure 7. Component stiffness and deformed shapes of the M1 connector system. Note: 1 in. = 25.4 mm; 1 ft = 0.305 m; 1 lb = 4.448 N.

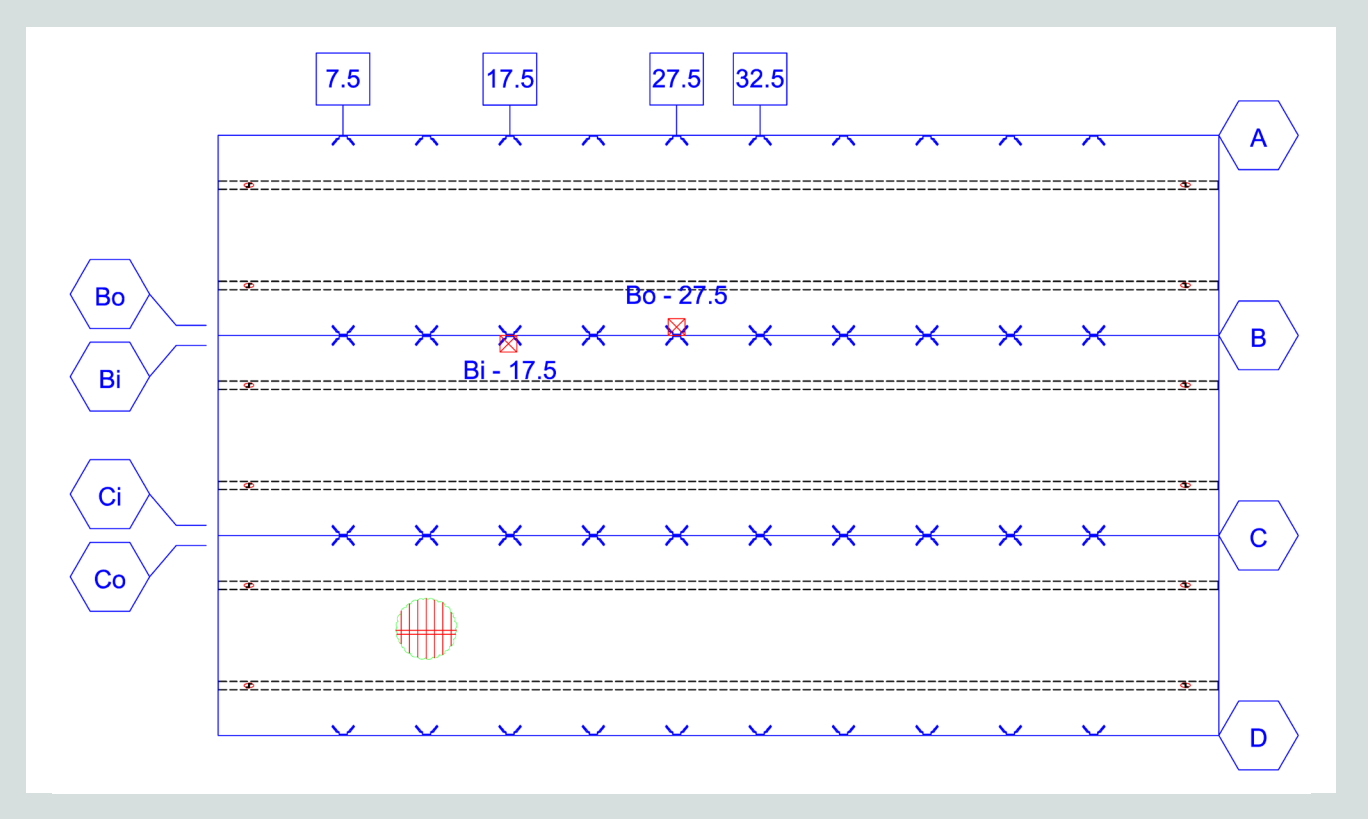

Figure 8. Full-scale double-tee setup. Note: All measurements are in feet. 1 ft = 0.305 m.

legs were embedded in a block with linear elastic concrete material properties. The connector was attached to the concrete by nodal ties along the embedded legs. Contact between the connector faceplate and concrete was modeled as hard frictionless contact. The element types used in the combined model were identical to those used in the M1 single-sided model outlined previously. To facilitate application of the nodal displacement and rotations obtained from the shell model of the diaphragm, the top and bottom surface nodes of the modeled concrete block were constrained to rigid body motion relative to a reference point at midheight of the block immediately adjacent to the connector. The nodal displacements and rotations were applied directly to the concrete block reference point.

The stiffness components of the connector system were determined by subjecting the connector assemblies to the following load cases:

- vertical shear deflection, K1
- axial deflection, K2
- rotation about the weld longitudinal axis, K3

Figure A7 shows the physical interpretation of the stiffness components of the connector system. The force or moment in the connection was plotted as a function of the deflection or rotation and was found to be linear for small deflections. **Figure 7** shows the stiffness plots next to the corresponding deflected shape of the connector system.

Development and validation of two-dimensional shell model of diaphragm

The stiffness for each connector type obtained from the 3-D finite element models was used to represent the behavior of the connections in a shell model of the floor diaphragm. The stiffness was input as a linear uncoupled link at the location of each connection. The model was created using thin shell elements for both the double-tee deck and legs. A 4 in. (100 mm) thick flange was used, typical of a pretopped double tee. The double-tee stem width was assumed as constant to simplify the model, with the width chosen to match the gross moment of inertia of the section. **Figure A8** illustrates a model of a three-double-tee system.

Coupled shell model three-dimensional finite element model validation

The final step of the proposed modeling approach imparts the vehicular loads to the shell model, measures the connector link deformations, and applies these displacements to the 3-D finite element model of the connection. To verify the accuracy of this approach, the model was compared with experimental test results conducted on full-scale double tees by Lucier et al.[19] The experiment consisted of point load application to three double-tee beams positioned side by side. The test setup comprised three 60 ft (18 m) 12DT30 double tees with the connectors along one joint from manufacturer 1 and the connectors along the other joint from manufacturer 2. The double-tee system

Table 2. Connector forces and differential deflections from finite element model

Load case	Estimated connector force at load point, lb	Estimated differential deflection, in.	Measured differential deflection for three load cases (average), in.
Bo-17.5	610	0.003	0.004, 0.0040, 0.004 (0.004)
Bi-17.5	590	0.004	0.006, 0.006, 0.007 (0.006)
Bo-27.5	510	0.003	0.001, 0.003, 0.002 (0.002)
B-27.5i	520	0.004	0.006, 0.003, 0.005 (0.005)
Bo-30.0	n/a	0.009	0.007, 0.008, 0.008 (0.008)
Bi-30.0	n/a	0.010	0.014, 0.015, 0.015 (0.014)

Note: n/a = not applicable. 1 in. = 25.4 mm; 1 lb = 4.448 N.

was subjected to point loads at various selected locations to determine the system response. During each load case, global deflections were monitored in nine locations and the strain response of five locations on several connectors was measured. Point loads up to 3000 lb (13,300 N) were applied to the double tees on each side of, and directly adjacent to, each connector.

The connectors on each side of the middle double tee were designated along lines B and C, with M1 connectors on line B and M2 connectors on line C. Load cases were designated as Bi, Bo, Ci, and Co, where Bi represents loading on the inside of connector line B and Bo represents loading on the outside of connector line B. Connectors were also labeled by their location along the length of the double tee in feet. For example, load case Bo-27.5 indicates that the load was applied on the outside of connector joint B at the connector located 27.5 ft (8.38 m) from the end of the double tee. **Figure 8** illustrates the double-tee layout and loading locations examined in this paper. Details of the test setup (**Fig. A9**) and results are presented in detail in Lucier et al.[19] Data gleaned from the tests were used to develop and refine the detailed finite element models and the iterative approach presented here.

A shell model of the full-scale test was developed. A modulus of elasticity of 4400 ksi (30 GPa) and Poisson's ratio of 0.15 were used for the concrete. The boundary conditions of the diaphragm included a longitudinal spring at bearing support with an axial stiffness of 107 kip/in. (18.74 kN/mm) to match the restraints observed in elastic tests of the double tee.

Determine shear force and relative deflections in connections

The shell element model of the test setup was compared with measured deformations for six load cases. A 1.5 kip (6.7 kN) point load was applied at six load patches to determine the estimated deformation across the joint adjacent to the load. **Table 2** summarizes a comparison of the model and measured deformations. As noted, three load cycles were applied to the double-tee panels. Significant variation was observed in the test between each load application; however, the model provides a comparable estimate of deformation.

To further validate the model, the relative deformations from the diaphragm model were applied to the detailed 3-D finite

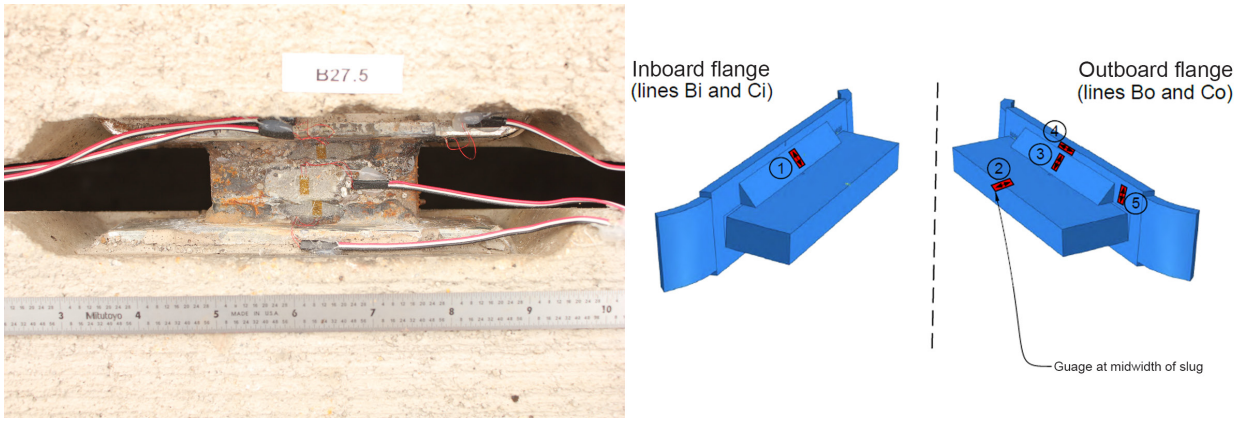

Figure 9. Photograph of connector B27.5 and schematic of strain gauge locations.

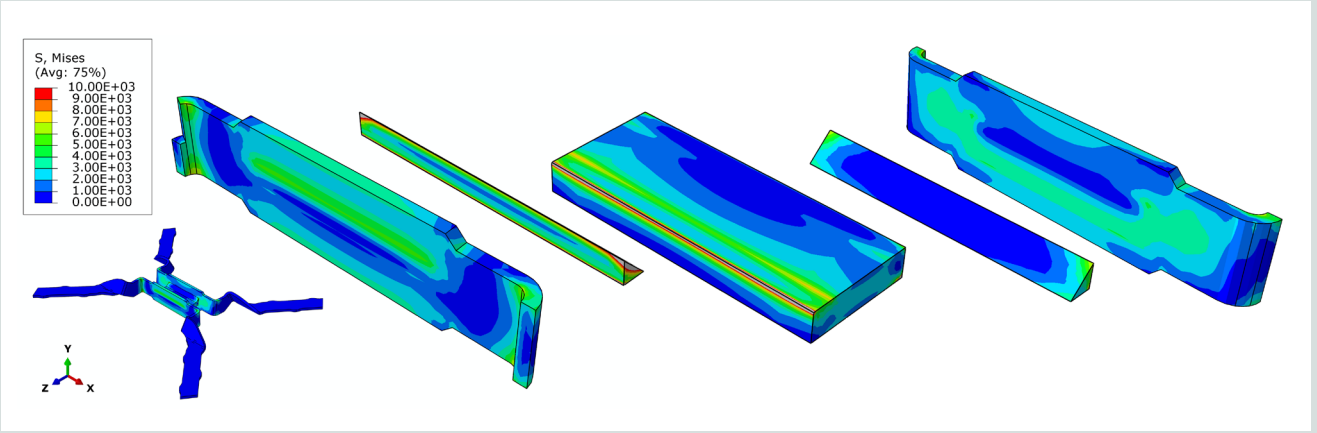

Figure 10. Von Mises stress distribution through connection.

element model of the connector system. The measured and modeled strains were compared for the Bo-27.5 load case. Five strain gauges (SG1–SG5) were installed at the connections (**Fig. 9**). The comparison was made by bounding the measured strains from gauges SG2, SG4, and SG5 between the nodal strains from the analysis taken in the region where the strain gauges were applied (**Fig. A10**). The strain varies significantly over the length of the strain gauge in these regions. Consequently, the range of finite element values in the region were compared with the measured strain gauge data. The measured strains were mostly bounded by the finite element model, indicating that the modeling approach is an adequate representation of the mechanics of the real system.

Determination of stress distribution in connection

The connection deformations determined from the shell model can be applied to the 3-D finite element model to assess the state of stress in the weld from the applied loading on the diaphragm. **Figure 10** illustrates the Von Mises stress at various components of the connection. The results indicate that under a point load application to the floor, the stress distribution in the connection varies considerably along the length of the weld and along the weld throat. Note the variation in Von Mises stress on the vertical face of the weld. The root of the weld on the downward deflected side (left) has a tensile stress, while the root of the weld on the side with the jumper plate in contact with the connector is in compression. The approach used in this study facilitates evaluation of the peak stresses in the connection, which can be used to assess fatigue life.

Case studies

To illustrate the application of the approach outlined in the paper, two case studies were conducted. The first examined the effect of weld penetration on the stresses in the weld, and the second examined the sensitivity of the connection to variations in double-tee size.

Influence of weld penetration on weld stress

Proprietary connections are typically designed with a draft on the faceplate, with the top of the faceplate leaning back into the flange. This design detail creates a V shape between adjacent connectors when the tees are installed. The V shape facilitates placement of jumper plates by minimizing the likelihood for the jumper plate to drop through to the floor below when installed for welding. The draft of the faceplate creates a gap between the top of the jumper plate and the faceplate (Fig. 3). During welding, this gap may or may not be filled with molten weld material. A section removed from the full-scale tests indicates that weld penetration is likely (**Fig. 11**). As illustrated, the amount of penetration can vary from a small amount to a quarter of the jumper plate depth (0.02 to 0.08 in.).

To examine the sensitivity to weld penetration, three 3-D finite element models are evaluated. The applied displacements and rotations were identical for all models, and the effects of weld penetration on the stiffness components of the connector were not examined. The welds in the previously modeled connections have been idealized as a triangular cross section. Actual field welding on connectors could be expected to have some penetration of weld metal into the gap between

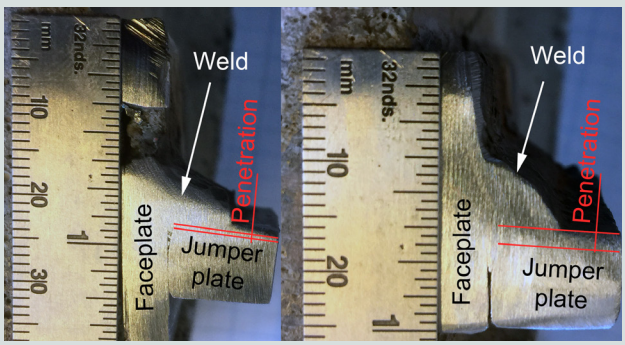

Figure 11. Weld penetration between jumper plate and faceplate.

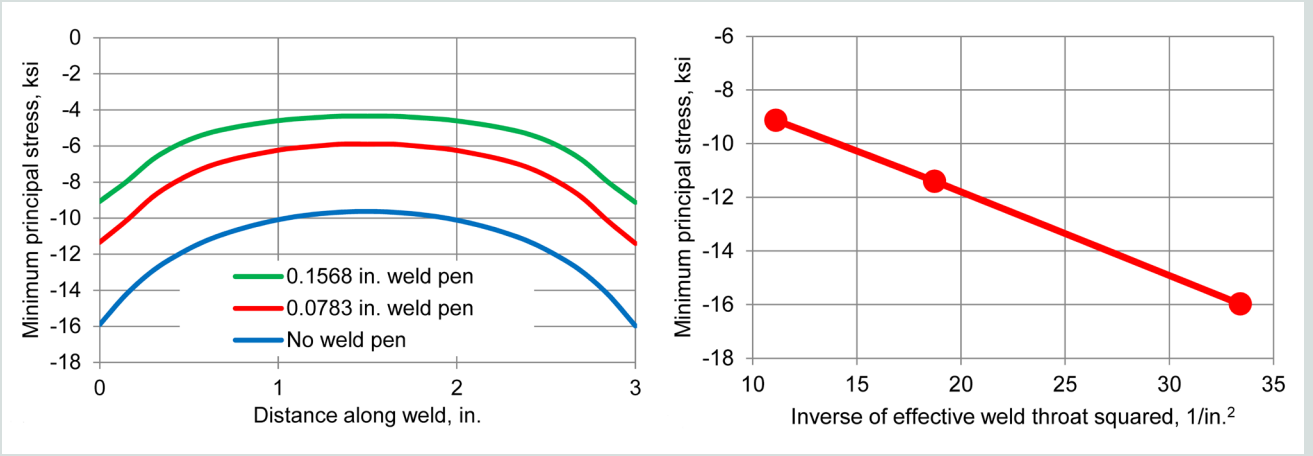

Figure 12. Variation of maximum principal stress at midface of weld with varying levels of weld penetration. Note: 1 in. = 25.4 mm; 1 ksi = 6.895 MPa.

the jumper plate and connector face due to the draft of the connector faceplate. The effects of weld penetration would be expected to decrease the stresses at the root of the weld for the same applied load. To illustrate this effect, the connection is modeled with three levels of penetration: no weld penetration (idealized triangular weld cross section), 0.0783 in. (2.0 mm) of penetration, and 0.1568 in. (4.0 mm) of penetration (**Fig. A11**).

Penetration of weld metal into the jumper plate/faceplate gap increases the effective throat of the fillet weld and consequently reduces the stress levels in the weld. **Figure 12** shows the maximum principal stress distribution along the weld at the centerline of the weld face. The analysis indicates that the principal stress level at the midsurface of the weld varies linearly as a function of the inverse of the effective throat length squared, where the effective throat is measured as the diagonal distance from the weld root to the centerline of the face of the weld (Fig. 12). A comparison of the strains recorded for gauge SG3 (Fig. 8) during load case Bo-27.5 shows that increasing the level of weld penetration causes the modeled strain to more closely match that measured during the test (**Fig. A12**). Analytical predictions are shown as ranges because the strain varies over the size of the strain gauge used in the test. For load case Bo-27.5, gauge SG3 is on the side of the connection where the weld root is in tension (the gap between the connector face and jumper plate is opening). Gauge SG1 is on the closing side of the connection and measured essentially no strain. This result correlates well with the model, which predicts effectively no strain at the weld face regardless of the level of weld penetration. The correlation between lower weld stress levels and weld penetration is an important aspect in assessing the fatigue life of these connections.

Influence of double-tee size on connections

A case study was conducted to examine the effect of double-tee size on the relative connection forces and stresses. Three double tees were examined: 10DT34, 12DT30, and 15DT30. The connection spacing for each double tee matched that of the full-scale tests (Lucier et al.[19]). **Figure 13** shows the relative double-tee sizes. The model consisted of three side-by-side double tees with M1 connectors. The jumper plate size was 3 × 1 × ⅜ in. (75 × 25 × 9.5 mm), and the mid-height of the jumper plate was at the midheight of the flange. The fillet weld size on both sides of the connection was ¼ in. (6 mm) and was 2.5 in. (64 mm) long, as recommended by the connector manufacturer. This connector configuration corresponds to the connector component stiffness analysis in Fig. A7.

The selected applied load was developed from a U.S. Environmental Protection Agency study on vehicle trends.[20] The average 2015 production vehicle (average of all trucks and cars) was chosen. The average weight of the vehicle is 4035 lb (17,950 N), including a 300 lb (1300 N) occupant load. The average footprint (wheel base by track width) was 49.4 ft^2 (4.59 m^2). Assuming a wheel base–to–track width ratio of approximately 1.6 and averaging to the nearest inch resulted in four point loads placed at a track width of 66 in. (1680 mm) and a wheel base of 105 in. (2670 mm). Assuming load is equally distributed to the four tires results in a 1009 lb (4488 N) point load at each location. This idealized vehicle was placed with the centerline of the wheels 3.0 in. (75 mm) from the joint, with the vehicle straddling the midspan of the double tee. This loading configuration puts the front wheels just outside the two connectors closest to the double-tee midspan and represents a near-worst-case loading scenario. As illustrated, the connection force magnitude is most sensitive to local bending of the free edge of the flange and varies as a function of the inverse cube of the free flange length (the distance between the double-tee stem and the free edge of the flange [Fig. 13 and **A13**]). This conclusion is supported by the observation that as the moment of inertia increases from the 12DT30 to the 15DT30, the connection forces also increase. Furthermore, as the distance from the stem to the edge of the tee decreases from the 15DT30 to the 12DT30 to the 10DT34,

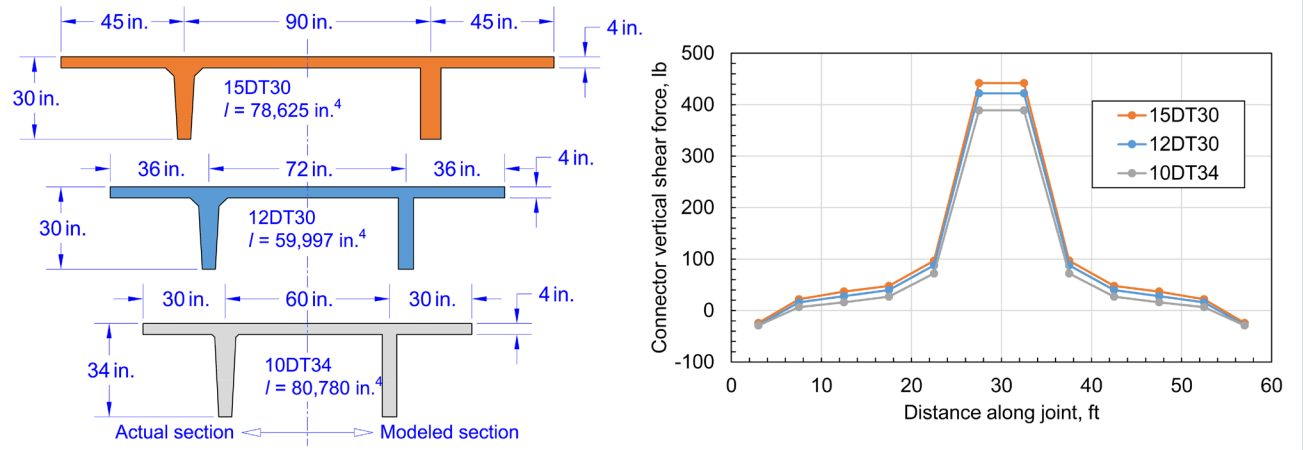

Figure 13. Connection force distribution in shell model for different double-tee sizes. Note: DT = double tee. 1 in. = 25.4 mm; 1 ft = 0.305 m; 1 lb = 4.448 N.

the local flange stiffness (that is, the bending resistance of the cantilever flange relative to the stem) increases as demonstrated by the increase in both principal stress and connection force (**Fig. A14** and **Table 3**). This increase in local flange stiffness results in an increased load being carried by global flexure of the loaded span with less force being transferred across all connections. Further parametric studies can be readily conducted with this method.

Conclusion

To properly assess the fatigue resistance of the connection requires a knowledge of the following:

- the relationship between the applied vehicle load and the resulting stresses in the connection welds
- dimensions of welds, including penetration, and jumper plate width
- the expected vehicle demands and distributions imposed on the structure over the expected service life
- an S-N curve that is applicable for the weld being considered

A numerical and experimental study was conducted to examine the first part. An iterative numerical method is proposed that consists of detailed 3-D finite element analysis of the connection and surrounding embedment with a parallel shell element model of the diaphragm. Based on the work, the following conclusions can be made:

- The stress in the weld cannot be determined by simplified engineering assumptions and requires finite element analysis methods to accurately determine the magnitude and distribution.
- The modeling methods are shown to accurately capture the complex mechanics of the connector system by comparison with test data.
- The connector stresses are dependent on the specific connector configuration, including the connector type, jumper plate dimensions, weld dimensions, and jumper plate width.
- The force level and corresponding connection stresses are influenced by local bending of the double-tee flange, which varies as a function of the inverse cube of the free flange length. Thus, modeling must account for the double-tee properties of the diaphragm system, especially the free flange length.
- The stresses in the welds can vary significantly depending on the extent of weld metal penetration into the gap

Table 3. Estimated response for case study

Double-tee size	Axial deformation, in.	Shear deformation, in.	Rotation on load side, rad	Rotation on other side, rad	Shear force in connection, lb-ft	Minimum principal stress, ksi
10DT34	0.00061	0.00260	0.00028	-0.00065	389	-13.9834
12DT30	0.00040	0.00280	0.00040	-0.00085	422	-16.6855
15DT30	0.00004	0.00300	0.00420	-0.00810	442	-17.8617

Note: 1 in. = 25.4 mm; 1 lb-ft = 1.356 N-m; 1 ksi = 6.895 MPa.

between the jumper plate and the connector. Weld penetration increases the effective throat length of the weld and the stress level varies with the square of the effective throat length. Failure to account for weld penetration will result in a significant overestimation of weld stresses.

- The methods outlined here, when combined with an accurate vehicular loading spectrum and appropriate fatigue-life curve for fillet welds subject to tension at the root, will allow for accurate fatigue-life analysis of precast concrete double-tee systems.

Acknowledgments

The authors would like to recognize that the experimental studies conducted as part of the research effort were funded by PCI. Connector hardware material was donated by several manufacturers. Many individuals contributed to the research effort, including Roger Becker, Ned Cleland, Larbi Sennour, Harry Gleich, Chuck Wynings, Chuck Magnesio, Eisa Rahmani, and Steven Altstadt.

References

1. Oliva, M. G. 2000. *Testing of the JVI Flange Connector for Precast Concrete Double-Tee Systems*. Structural Materials and Testing Lab report, University of Wisconsin, Madison, WI.

2. Venuti, W. J. 1970. "Diaphragm Shear Connectors between Flanges of Prestressed Concrete T-Beams." *PCI Journal* 15 (1): 67–78.

3. Spencer, R. A., and D. S. Neille. 1976. "Cyclic Tests of Welded Headed Stud Connections." *PCI Journal* 21 (3): 70–83.

4. Aswad, A. 1977. *Comprehensive Report on Precast and Prestressed Connectors Testing Program*. Denver, CO: Stanley Structures.

5. Pincheira, J. A., M. G. Oliva, and F. I. Kusumo-Rahardjo. 1998. "Tests on Double Tee Flange Connectors Subjected to Monotonic and Cyclic Loading." *PCI Journal* 43 (3): 82–96.

6. Oliva, M. G. 2000. *Testing of the JVI Flange Connector for Precast Concrete Double-Tee Systems*. Structural Materials and Testing Lab report, University of Wisconsin, Madison, WI.

7. Wiss, Janney, Elstner Associates. 2002. *Dayton/Richmond Flange-to-Flange Connector Tests*. Northbrook, IL: Wiss, Janney, Elstner Associates.

8. Shaikh, F. A., and E. P. Feile. 2004. "Load Testing of a Precast Concrete Double-Tee Flange Connector." *PCI Journal* 49 (3), 84–95.

9. Naito, C. 2007. *Erector Connector Meadow Burke Company In-Plane Performance*. ATLSS report 06-22. Bethlehem, PA: Lehigh University.

10. Naito, C., and R. Hendricks. 2008. *In-Plane and Out-of-Plane Performance of the MC Flange Connector*. ATLSS report 08-08. Bethlehem, PA: Lehigh University.

11. Ren, R., and C. Naito. 2013. "Precast Concrete Diaphragm Connector Performance Database." *Journal of Structural Engineering* 139 (1): 15–27.

12. Naito, C., L. Cao, and W. Peter. 2009. "Precast Concrete Double-Tee Connections, Part 1: Tension Behavior." *PCI Journal* 54 (1): 49–66.

13. Cao, L., and C. Naito. 2009. "Precast Concrete Double-Tee Connections, Part 2: Shear Behavior." *PCI Journal* 54 (2): 97–115.

14. Naito, C., and R. Ren. 2013. "An Evaluation Method for Precast Concrete Diaphragm Connectors Based on Structural Testing." *PCI Journal* 58 (2): 106–118.

15. Klein, G., and R. Lindenberg. 2009. *Volume Change Movement and Forces in Precast Concrete Buildings*. Research report 2002.1117. Northbrook, IL: Wiss, Janney, Elstner Associates.

16. PCI Connections Details Committee. 2008. *PCI Connections Manual for Precast and Prestressed Concrete Construction*. MNL-138-08. Chicago, IL: PCI.

17. ASTM Subcommittee C09.61. 2014. *Standard Test Method for Compressive Strength of Cylindrical Concrete Specimens*. ASTM C39/C39M-04. West Conshohocken, PA: ASTM International.

18. Naito, C., and R. Hendricks. 2016. "PCI Fatigue Study: Experimental Evaluation of Double Tee Flange Connectors Subject to Out-of-Plane Loading." ATLSS report 16-07. Bethlehem, PA: Lehigh University.

19. Lucier, G., C. Naito, A. Osborn, M. Nafadi, and S. Rizkalla. 2017. "Double Tee Flange Connections—Experimental Evaluation." Paper 98 presented at PCI Convention and National Bridge Conference, Cleveland, OH, Feb. 28–Mar. 4.

20. United States Environmental Protection Agency. 2016. *Light-Duty Automotive Technology, Carbon Dioxide Emissions, and Fuel Economy Trends: 1975 Through 2016*. EPA-420-R-16-010. doi:10.1002/yd.282

About the authors

Robin Hendricks is a research engineer with the ATLSS Center at Lehigh University in Bethlehem, Pa.

Clay Naito is a professor in the Department of Civil Engineering at Lehigh University.

Andrew Osborn is senior principal at Wiss, Janney, Elstner Associates in Boston, Mass.

Abstract

A PCI-funded research effort was conducted to assess the fatigue resistance of welded flange-to-flange connections used in double-tee precast concrete construction. The connection consists of steel connectors embedded in the edges of adjacent precast concrete double-tee flanges welded together using a steel jumper plate and fillet welds. Variations of this connection have been used for over 50 years with success. The strength limit states of this connection have been explored in detail, but the stresses in the connection at cyclic service load levels are not well understood. The research effort presented here was conducted specifically to quantify the fatigue resistance of these connections to the repeated loading typical of parking structure service demands. A two-part series of articles was developed to summarize methods that can be used to accurately analyze and assess the fatigue life of these connections. This paper examines numerical methods that can be used to determine the state of stress in the weld under service loads. The ability to accurately determine the stresses in the weld can be combined with a vehicular load spectrum and a suitable fatigue-life curve for the fillet weld detail to obtain a realistic assessment of the fatigue life of connections.

Keywords

Connection, diaphragm, double tee, fatigue, finite element model, service life, stiffness, stress, vehicle, weld penetration.

Review policy

This paper was reviewed in accordance with the Precast/Prestressed Concrete Institute's peer-review process.

Reader comments

Please address any reader comments to *PCI Journal* editor-in-chief Emily Lorenz at elorenz@pci.org or Precast/Prestressed Concrete Institute, c/o *PCI Journal*, 200 W. Adams St., Suite 2100, Chicago, IL 60606.